Optical Forces and Torques in Nonuniform Beams of Light

David B. Ruffner and David G. Grier

Phys. Rev. Lett. **108**, 173602 — Published 24 April 2012

DOI: 10.1103/PhysRevLett.108.173602

Optical forces and torques in non-uniform beams of light

David B. Ruffner and David G. Grier
Department of Physics and Center for Soft Matter Research, New York University, New York, NY 10003

The spin angular momentum in an elliptically polarized beam of light plays several noteworthy roles in optical traps. It contributes to the linear momentum density in a non-uniform beam, and thus to the radiation pressure exerted on illuminated objects. It can be converted into orbital angular momentum, and thus can exert torques even on optically isotropic objects. Its curl, moreover, contributes to both forces and torques without spin-to-orbit conversion. We demonstrate these effects experimentally by tracking colloidal spheres diffusing in elliptically polarized optical tweezers. Clusters of spheres circulate deterministically about the beam's axis. A single sphere, by contrast, undergoes stochastic Brownian vortex circulation that maps out the optical force field.

Optical forces arising from the polarization and polarization gradients in vector beams of light constitute a new frontier for optical micromanipulation. Linearly polarized light has been used to orient birefringent objects in conventional optical tweezers [1–3] and circular polarization has been used to make them rotate [1, 3–7]. More recently, optically isotropic objects also have been observed to circulate in circularly polarized optical traps [8–10], through a process described as spin-to-orbit conversion [10–14]. Here, we present a general formulation of the linear and angular momentum densities in vector beams of light that clarifies how the amplitude, phase and polarization profiles contribute to the forces and torques that such beams exert on illuminated objects. This formulation reveals that the curl of the spin angular momentum can exert torques on illuminated objects without contributing to the light's orbital angular momentum, and that this effect dominates spin-to-orbit conversion in circularly polarized optical tweezers. Predicted properties of polarization-dependent optical forces are confirmed through observations of a previously unreported mode of Brownian vortex circulation for an isotropic sphere in elliptically polarized optical tweezers.

The vector potential describing a monochromatic beam of light of angular frequency ω may be written as

$$\boldsymbol{A}(\boldsymbol{r},t) = u(\boldsymbol{r})\; e^{i\,\varphi(\boldsymbol{r})-i\omega t}\,\hat{\boldsymbol{\epsilon}}(\boldsymbol{r})\,, \tag{1}$$

where $u(\boldsymbol{r})$ is the real-valued amplitude, $\varphi(\boldsymbol{r})$ is the real-valued phase and $\hat{\boldsymbol{\epsilon}}(\boldsymbol{r})$ is the complex-valued polarization vector at position $\boldsymbol{r}$. This description is useful for practical applications because $u(\boldsymbol{r})$, $\varphi(\boldsymbol{r})$ and $\hat{\boldsymbol{\epsilon}}(\boldsymbol{r})$ may be specified independently, for example using holographic techniques [3, 15–17]. Poynting's theorem then yields the time-averaged momentum density

$$\boldsymbol{g}(\boldsymbol{r}) = \frac{\omega}{2\mu c^2}\,\Im\left\{\boldsymbol{A}^*(\boldsymbol{r},t)\times\left[\nabla\times\boldsymbol{A}(\boldsymbol{r},t)\right]\right\}, \tag{2}$$

where μ is the permeability of the medium and c is the speed of light in the medium. The momentum density gives rise to the radiation pressure that the light exerts on illuminated objects and may be expressed in terms of the experimentally accessible parameters as

$$\boldsymbol{g}(\boldsymbol{r}) = \frac{\omega}{2\mu c^2}\,I(\boldsymbol{r})\;\nabla\varphi - \frac{i\omega}{2\mu c^2}\,I(\boldsymbol{r})\;\epsilon_j^*\nabla\epsilon_j + \frac{1}{2}\nabla\times\boldsymbol{s}, \tag{3}$$

where $I(\boldsymbol{r}) = u^2(\boldsymbol{r})$ is the intensity and where

$$\boldsymbol{s}(\boldsymbol{r}) = \frac{\omega}{2\,\mu c^2}\,I(\boldsymbol{r})\;\boldsymbol{\sigma}(\boldsymbol{r}) \tag{4}$$

is the spin angular momentum density in a beam of light with local helicity

$$\boldsymbol{\sigma}(\boldsymbol{r}) = i\,\hat{\boldsymbol{\epsilon}}(\boldsymbol{r})\times\hat{\boldsymbol{\epsilon}}^*(\boldsymbol{r})\,. \tag{5}$$

The projection of $\boldsymbol{\sigma}(\boldsymbol{r})$ onto the propagation direction $\hat{k}(\boldsymbol{r})$ is related to the Stokes parameters of the beam [18] by $\boldsymbol{\sigma}(\boldsymbol{r})\cdot\hat{k}(\boldsymbol{r}) = S_3(\boldsymbol{r})/S_0(\boldsymbol{r})$. It achieves extremal values of $+1$ and -1 for right- and left-circularly polarized light, respectively.

The momentum density described by Eq. (3) gives rise to the radiation pressure experienced by objects that absorb or scatter light. Identifying $\boldsymbol{g}(\boldsymbol{r})$ with the radiation pressure on a particle is most appropriate in the Rayleigh limit, when the particle's size is no greater than the wavelength of light. In this limit, the three terms in $\boldsymbol{g}(\boldsymbol{r})$ may be interpreted as distinct mechanisms by which a beam of light exerts forces on illuminated objects.

The first two terms in Eq. (3) constitute the familiar phase-gradient contribution to the radiation pressure [16]. In this context, the second term accounts for the independent phase profiles that may be imposed on the real and imaginary components of the polarization in an elliptically polarized beam. Phase gradients have been used to create three-dimensional optical force landscapes [16], such as knotted force fields [19] and true tractor beams [20]. They also account for the orbital angular momentum density

$$\boldsymbol{\ell}(\boldsymbol{r}) = \frac{\omega}{2\mu c^2}\,I(\boldsymbol{r})\;\left[\boldsymbol{r}\times\left(\nabla\varphi - i\epsilon_j^*\nabla\epsilon_j\right)\right], \tag{6}$$

carried by helical modes of light [21, 22]. In this context, the polarization-dependent term in Eq. (6) vanishes identically in linearly polarized light, but manifests spin-to-orbit conversion in elliptically polarized beams.

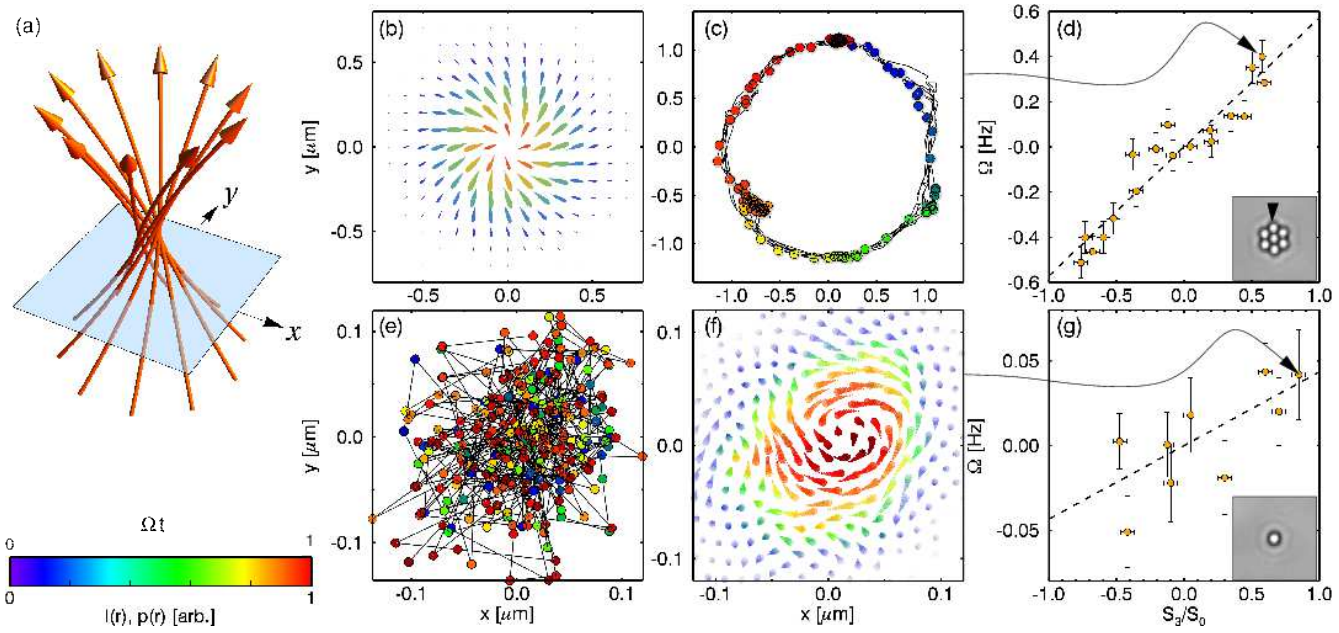

FIG. 1: (Color online) (a) Streamlines of the momentum density $\boldsymbol{g}(\boldsymbol{r})$ in a right-circularly polarized optical tweezer. (b) Components of $\boldsymbol{g}(\boldsymbol{r})$ in the plane indicated in (a), shaded by the intensity $I(\boldsymbol{r})$. (c) Measured trajectory of one particle in a seven-sphere cluster trapped near the focus of the beam. Discrete points show the last three seconds of motion, colored by time. (d) Circulation rate Ω as a function of the beam's Stokes parameters S_3/S_0. Inset: snapshot of the cluster indicating the sphere whose trajectory is plotted. (e) Three seconds of a 3.5-minute trajectory of a single polystyrene sphere diffusing in a circularly polarized optical tweezer, shaded by time. (f) Time-averaged probability flux $\boldsymbol{j}(\boldsymbol{r})$ computed from the full measured trajectory. Barbs are colored by the relative probability density $p(\boldsymbol{r})$ computed from the same trajectory. Brownian vortex circulation is apparent in the vorticity of $\boldsymbol{j}(\boldsymbol{r})$. (g) Dependence of the Brownian vortex circulation rate on S_3/S_0. Inset: snapshot of the trapped sphere. The color bar indicates relative intensity $I(\boldsymbol{r})$ for (b), time for (c) and (e), and relative probability $p(\boldsymbol{r})$ for (f).

The third term in Eq. (3) describes how variations in spin angular momentum contribute to the linear momentum density in non-uniform beams of light. This spin-curl term encompasses forces due to spatially-varying elliptical polarization and also those due to intensity variations in elliptically polarized beams. Streamlines of $\nabla \times \boldsymbol{s}$ naturally loop around extrema in the beam's intensity. Spin-curl forces thus tend to make illuminated objects circulate in the plane transverse to the direction of propagation. Observations of colloidal spheres circulating in beams of light with spatially-varying elliptical polarization [10, 13, 23] consequently have been interpreted as evidence that the curl of the polarization contributes to the light's orbital angular momentum. Equation (6), however, makes clear that the spin-curl contribution to $\boldsymbol{g}(\boldsymbol{r})$ does not contribute in any way to $\boldsymbol{\ell}(\boldsymbol{r})$. For the same reason, observations of optically-induced circulation in uniformly circularly-polarized optical traps [8, 9] need not imply spin-to-orbit conversion.

To illustrate these point, we consider the forces exerted on an optically isotropic colloidal sphere by elliptically polarized optical tweezers. We model the trap as an Gaussian beam of wavenumber k brought to a focus with convergence angle α by a lens of focal length f and numerical aperture $NA = n_m \sin\alpha$ in a medium of refractive index n_m. The beam's initial polarization is

$$\hat{\boldsymbol{\epsilon}}(\boldsymbol{r}) = \frac{1}{\sqrt{2}} \left(\hat{\boldsymbol{x}} + e^{i\delta}\, \hat{\boldsymbol{y}} \right), \tag{7}$$

with a corresponding incident helicity $\sigma_0 = \sin\delta$ along $\hat{\boldsymbol{z}}$. The focused beam's vector potential may be expressed in cylindrical coordinates $\boldsymbol{r} = (\rho, \phi, z)$ with the Richards-Wolf integral formulation [14, 24, 25],

$$\begin{aligned} \boldsymbol{A}(\boldsymbol{r}) = &-i\, [A_0(\boldsymbol{r}) + A_2(\boldsymbol{r})] \left(\cos\phi + e^{i\delta} \sin\phi \right) \hat{\rho} \\ &- i\, [A_0(\boldsymbol{r}) - A_2(\boldsymbol{r})] \left(e^{i\delta} \cos\phi - \sin\phi \right) \hat{\phi} \\ &- 2\, A_1(\boldsymbol{r}) \left(\cos\phi + e^{i\delta} \sin\phi \right) \hat{z}, \end{aligned} \tag{8}$$

as a Fourier-Bessel expansion

$$A_n(\boldsymbol{r}) = \frac{kfu_0}{2i\omega} \int_0^{\alpha} a_n(\theta)\, J_n(k\rho \sin\theta)\, e^{izk\cos\theta}\, d\theta, \tag{9}$$

with expansion coefficients [25]

$$a_0(\theta) = (1 + \cos\theta)\, \sin\theta \sqrt{\cos\theta} \tag{10}$$

$$a_1(\theta) = \sin^2\theta\, \sqrt{\cos\theta} \tag{11}$$

$$a_2(\theta) = (1 - \cos\theta)\, \sin\theta\, \sqrt{\cos\theta}. \tag{12}$$

Streamlines of $\boldsymbol{g}(\boldsymbol{r})$ in a right-circularly polarized optical tweezer ($\sigma_0 = +1$, NA = 1.4) are shown spiraling around the optical axis in Fig. 1(a).

A slice through the beam in the transverse plane indicated in Fig. 1(a) reveals the azimuthal component to the transverse momentum density $g_\perp(\boldsymbol{r}) = \boldsymbol{g}(\boldsymbol{r}) \cdot \hat{\phi}$ that is plotted in Fig. (1b). The transverse momentum density may be resolved into two contributions

$$g_\perp(\boldsymbol{r}) = g_O(\boldsymbol{r}) + g_S(\boldsymbol{r}) \tag{13}$$

arising from the spin-to-orbit and spin-curl contributions to $\boldsymbol{g}(\boldsymbol{r})$, respectively:

$$g_O(\boldsymbol{r}) = \frac{2\omega}{\mu c^2}\,\frac{1}{\rho}\,\left[|A_1(\boldsymbol{r})|^2 + |A_2(\boldsymbol{r})|^2\right]\,\sigma_0 \quad \text{and} \tag{14}$$

$$g_S(\boldsymbol{r}) = \frac{\omega}{\mu c^2}\,\left[\partial_z \Im\left\{A_1^*(\boldsymbol{r})\,\left(A_0(\boldsymbol{r}) - A_2(\boldsymbol{r})\right)\right\} - \partial_r\left(|A_0(\boldsymbol{r})|^2 - |A_2(\boldsymbol{r})|^2\right)\right]\,\sigma_0. \tag{15}$$

Both are proportional to the helicity of the incident beam, σ_0. They do not, however, contribute equally to the transverse component of the radiation pressure. At the focus of the circularly-polarized optical tweezer, for example, 79% of the transverse momentum density is due to the spin-curl term $g_S(\boldsymbol{r})$ and only 21% from spin-to-orbit conversion. More generally, both $A_1(\boldsymbol{r})$ and $A_2(\boldsymbol{r})$ vanish in the paraxial approximation; there is no spin-to-orbit conversion in weakly focused beams. The spin-curl contribution, by contrast, persists in the paraxial limit.

We probe the properties of spin-dependent optical forces by measuring their influence on the motion of micrometer-scale colloidal spheres. Our system consists of 1.0 μm diameter polystyrene (PS) spheres (Polysciences, Lot # 586632) dispersed in water and trapped in optical tweezers whose helicity σ_0 is controlled with a quarter-wave plate. The isotropic dielectric spheres absorb very little light directly. By scattering light, however, they experience radiation pressure proportional to the local momentum density. Our optical tweezer is powered by up to 4 Wof laser light at a vacuum wavelength of $\lambda = 532$ nm (Coherent Verdi 5W). The elliptically polarized beam is relayed with a dichroic mirror to the input pupil of an objective lens (Nikon Plan Apo, 100×, NA 1.4), which focuses the light into a trap. We account for the mirror's influence on the polarization by measuring the beam's Stokes parameters in the input plane of the objective lens. The sample is imaged using the same lens in conventional bright-field illumination, which passes through the dichroic mirror to a video camera (NEC TI-324AII). Digitally recorded video is analyzed with standard methods of digital video microscopy [26] to measure the trajectory $\boldsymbol{r}_j = \boldsymbol{r}(j\tau)$ of a probe particle with 10 nmresolution at $\tau = 33$ ms intervals.

The trajectory plotted in Fig. 1(c) was obtained for one of seven spheres trapped against a glass surface by a right-circularly-polarized optical tweezer ($\sigma_0 = +0.8$) powered by 1.5 W. The optically-assembled cluster, shown inset into Fig. 1(d), spans the region of the beam indicated in Fig. 1(b), and thus rotates about the beam axis at a rate of roughly $\Omega = 0.4$ Hz. The data in Fig. 1(d) confirm the prediction of Eqs. (14) and (15) that the rotation rate varies linearly with the degree of circular polarization.

The colloidal cluster circulates deterministically in the elliptically polarized optical tweezer because it continuously scatters light in regions where $g_\perp(\boldsymbol{r})$ is substantial. A single sphere diffusing in an elliptically polarized optical tweezer, by contrast, explores the entire force landscape presented by the light. This includes regions near the optical axis where $g_\perp(\boldsymbol{r})$ is predicted to vanish. Figure 1(e) shows the measured trajectory of one such sphere in a right-circularly-polarized trap ($\sigma_0 = +0.8$) powered by 0.05 W. Optically-induced circulation is not immediately obvious in the noisy trajectory, which is shaded to indicate the passage of time. It becomes evident when the trajectory $\boldsymbol{r}_j$ is compiled into a time-averaged estimate [27] for the steady-state probability current

$$\boldsymbol{j}(\boldsymbol{r}) = \frac{1}{N-1}\,\sum_{j=1}^{N-1}\,\frac{\boldsymbol{r}_{j+1} - \boldsymbol{r}_j}{\tau}\,\delta_{\sigma_j}\left(\boldsymbol{r} - \frac{\boldsymbol{r}_{j+1} + \boldsymbol{r}_j}{2}\right), \tag{16}$$

which is plotted in Fig. 1(f). Here $N = 7,000$ is the number of discrete samples, and $\delta_\sigma(\boldsymbol{r})$ is the kernel of an adaptive density estimator [27] whose width σ varies with the sampling density. The symbols in Fig. 1(f) are shaded by the estimated probability density

$$p(\boldsymbol{r}) = \frac{1}{N}\,\sum_{j=1}^{N}\,\delta_{\sigma_j}(\boldsymbol{r} - \boldsymbol{r}_j) \tag{17}$$

for finding the particle near $\boldsymbol{r}$. Together, $\boldsymbol{j}(\boldsymbol{r})$ and $p(\boldsymbol{r})$ confirm the prediction of Eqs. (14) and (15) that circulation vanishes on the optical axis where the particle's probability density is greatest.

Taking care to measure $\boldsymbol{r}$ from the center of circulation, the mean circulation rate may be estimated as

$$\Omega = \int \rho(\boldsymbol{r})\,\left[\boldsymbol{r} \times \boldsymbol{j}(\boldsymbol{r})\right] \cdot \hat{\boldsymbol{z}}\,d^2r. \tag{18}$$

Equation (18) improves upon the graphical method for estimating Ω introduced in Ref. [28] by making optimal use of discretely sampled data [27]. Because the single particle spends most of its time in a curl-free region of the optical force field, its circulation rate is substantially smaller than in the deterministic case. Even so, the data in Fig. 1(g) again are consistent with the prediction that Ω scales linearly with σ_0.

The single particle's stochastic motion differs qualitatively from the cluster's deterministic circulation. Were it not for random thermal forces, the isolated sphere would remain at mechanical equilibrium on the optical axis. Thermal forces enable it to explore the optical force landscape, where it is advected by the spin-dependent

contribution to the radiation pressure. This system, therefore constitutes an example of a Brownian vortex [29, 30], a stochastic machine that uses noise to transduce work out of a static non-conservative force field.

Unlike previous experimental demonstrations of Brownian vortexes [28, 29] the conservative restoring force in this system is transverse to the non-conservative contributions. Consequently, the particle's radial excursions are described by the Boltzmann distribution [30] $p(\boldsymbol{r}) = \exp\left(-\beta U(\boldsymbol{r})\right)$ where $\beta^{-1} = k_B T$ is the thermal energy scale at absolute temperature T and $U(\boldsymbol{r})$ is the particle's potential energy in the trap. The solenoidal part of the radiation pressure [30]

$$\boldsymbol{f}(\boldsymbol{r}) = \frac{\xi\omega}{8\pi\mu c^2}\,\nabla\times\int\frac{\nabla'\times I(\boldsymbol{r}')\left[\nabla'\varphi - i\hat{\boldsymbol{\epsilon}}_j^*\nabla'\hat{\boldsymbol{\epsilon}}_j\right]}{|\boldsymbol{r}-\boldsymbol{r}'|}\,d^3r' + \frac{\xi}{2}\,\nabla\times\boldsymbol{s}(\boldsymbol{r})\,, \quad (19)$$

then advects $p(\boldsymbol{r})$ into the probability current $\boldsymbol{j}(\boldsymbol{r}) = \mu_p p(\boldsymbol{r})\,\boldsymbol{f}(\boldsymbol{r})$, where ξ is the particle's scattering cross-section and μ_p is its mobility. The first term in Eq. (19) may be neglected in a beam such as a optical tweezer that carries little or no orbital angular momentum. The data in Fig. 1(f) thus map out the spin-curl force in the transverse plane. Moreover, because the circulation direction is determined unambiguously by the curl of $\boldsymbol{f}(\boldsymbol{r})$, this system is a practical realization of a so-called *trivial Brownian vortex*, which has been proposed [30] but not previously demonstrated.

Formulating the optical momentum density in terms of experimentally accessible parameters clarifies the nature and origin of the forces that can be applied to microscopic objects using the radiation pressure in beams of light. This formulation confirms previous reports of forces arising from phase gradients [16] and demonstrates that phase-gradient forces act independently of the state of polarization. The spin-curl mechanism unifies forces arising from the curl of the polarization and forces due to intensity gradients in elliptically polarized beams. Because they induce circulatory motion, spin-curl forces are easily misinterpreted as evidence for spin-to-orbit conversion. The spin-curl density, however, does not contribute to the orbital angular momentum of the light. Spin-to-orbit conversion, by contrast, removes spin angular momentum from a beam of light and transmutes it into orbital angular momentum [11]. The present formulation clarifies this mechanism, and reveals that spin-to-orbit conversion has played a secondary role in previous reports of optically-induced circulation. Using Eq. (3) as a guide, all three mechanisms now may be optimally leveraged to improve optical micromanipulation and the performance of light-driven machines.

We acknowledge helpful discussions with Giovanni Milione. This work was supported by the National Science Foundation principally through Grant Number DMR-0855741, and in part by Grant Number DMR-0922680.

[1] M. E. J. Friese, T. A. Nieminen, N. R. Heckenberg, and H. Rubinsztein-Dunlop, Nature **394**, 348 (1998).
[2] S. K. Mohanty, K. D. Rao, and P. K. Gupta, Appl. Phys. B **80**, 631 (2005).
[3] D. Preece, S. Keen, E. Botvinick, R. Bowman, M. Padgett, and J. Leach, Opt. Express **16**, 15897 (2008).
[4] A. T. ONeil and M. J. Padgett, Opt. Commun. **185**, 139 (2000).
[5] A. T. O'Neil, I. MacVicar, L. Allen, and M. J. Padgett, Phys. Rev. Lett. **88**, 053601 (2002).
[6] E. Santamato, B. Daino, M. Romagnoli, M. Settembre, and Y. R. Shen, Phys. Rev. Lett. **57**, 2423 (1986).
[7] A. I. Bishop, T. A. Nieminen, N. R. Heckenberg, and H. Rubinsztein-Dunlop, Phys. Rev. Lett. **92**, 198104 (2004).
[8] Y. Zhao, J. S. Edgar, G. D. M. Jeffries, D. McGloin, and D. T. Chiu, Phys. Rev. Lett. **99**, 073901 (2007).
[9] Y. Zhao, D. Shapiro, D. Mcgloin, D. T. Chiu, and S. Marchesini, Opt. Express **17**, 23316 (2009).
[10] X. L. Wang, J. Chen, Y. Li, J. Ding, C. S. Guo, and H. T. Wang, Phys. Rev. Lett. **105**, 253602 (2010).
[11] T. A. Nieminen, A. B. Stilgoe, N. R. Heckenberg, and H. Rubinsztein-Dunlop, J. Opt. A **10**, 115005 (2008).
[12] S. Yan, B. Yao, and M. Lei, Phys. Rev. Lett. **106**, 189301 (2011).
[13] X. L. Wang, J. Chen, Y. N. Li, J. P. Ding, C. S. Guo, and H. T. Wang, Phys. Rev. Lett. **106**, 189302 (2011).
[14] Z. Bomzon, M. Gu, and J. Shamir, Appl. Phys. Lett. **89**, 241104 (2006).
[15] D. G. Grier, Nature **424**, 810 (2003).
[16] Y. Roichman, B. Sun, Y. Roichman, J. Amato-Grill, and D. G. Grier, Phys. Rev. Lett. **100**, 013602 (2008).
[17] Q. Zhan, Adv. Opt. Phot. **1**, 1 (2009).
[18] M. Born and E. Wolf, *Principles of Optics* (Cambridge University Press, 1997), 6th ed.
[19] E. R. Shanblatt and D. G. Grier, Opt. Express **19**, 5833 (2011).
[20] S.-H. Lee, Y. Roichman, and D. G. Grier, Opt. Express **18**, 6988 (2010).
[21] L. Allen, M. W. Beijersbergen, R. J. C. Spreeuw, and J. P. Woerdman, Phys. Rev. A **45**, 8185 (1992).
[22] N. B. Simpson, L. Allen, and M. J. Padgett, J. Mod. Opt. **43**, 2485 (1996).
[23] G. Cipparrone, I. Ricardez-Vargas, P. Pagliusi, and C. Provenzano, Opt. Express **18**, 6008 (2010).
[24] E. Wolf, Proc. Royal Soc. London A **253**, 349 (1959).
[25] B. Richards and E. Wolf, Proc. Royal Soc. London. A **253**, 358 (1959).
[26] J. C. Crocker and D. G. Grier, J. Colloid Interface Sci. **179**, 298 (1996).
[27] B. W. Silverman, *Density Estimation for Statistics and Data Analysis* (Chapman and Hall/CRC, 1986), 1st ed.
[28] Y. Roichman, B. Sun, A. Stolarski, and D. G. Grier, Phys. Rev. Lett. **101**, 128301 (2008).
[29] B. Sun, J. Lin, E. Darby, A. Y. Grosberg, and D. G. Grier, Phys. Rev. E **80**, 010401 (2009).
[30] B. Sun, D. G. Grier, and A. Y. Grosberg, Phys. Rev. E **82**, 021123 (2010).